Critical test of CdTe(100) angle-resolved photoemission spectra with band-structure calculations

David W. Niles and Hartmut Höchst
Synchrotron Radiation Center, University of Wisconsin-Madison, 3731 Schneider Drive, Stoughton, Wisconsin 53589-3097
(Received 21 June 1990; revised manuscript received 7 September 1990)

Angle-resolved synchrotron-radiation photoemission spectroscopy was used to determine the spin-orbit splitting between the Γ_8 and Γ_7 valence bands and to map the dispersion $E(\mathbf{k})$ of the light- and heavy-hole bands as well as the split-off valence band along the [100] direction in CdTe. At a photon energy of $h\nu=10$ eV, we find that a direct transition from the Brillouin-zone center is possible only from the highest occupied Γ_8 valence band, while for $h\nu=11$ eV, the split-off Γ_7 band has comparable transition probability and also contributes to the normal-emission spectrum. The measured spin-orbit splitting $\Delta\varepsilon_{s.o.}=0.95$ eV is in agreement with values reported from optical measurements. The experimentally determined valence-band critical-point energies are $X_7 \leq -1.4$ eV, $X_6=-2.2$ eV, and $X_7=-4.4$ eV. A comparison of these data points as well as the dispersion behavior of the top three valence bands is made with results based upon nonlocal pseudopotential, tight-binding, and self-consistent local-density approximations.

I. INTRODUCTION

Optical-spectroscopy techniques such as electroreflectance provided the bulk of experimental data needed to understand the electronic band structures of semiconductors.[1] Based on the critical-point energies determined through measurements of group IV and many II-VI compound semiconductors, theoretical schemes were developed to calculate electronic band dispersions throughout the entire Brillouin zone. Among the various theoretical methods, relativistic othogonal-plane-wave (OPW) and empirical pseudopotential band calculations were by far the most successful in predicting characteristic valence- and conduction-band features as well as optical properties of many representative semiconducting materials.[2,3]

Even though optical spectroscopy has made enormous contributions to today's understanding of the electronic properties of solids, many optical measurements suffer from a shortcoming. They are differential techniques, and as such one can often not read energies directly from them. Recent studies indicate that electrorefelectance data which contain first- and second-order derivative components often do not allow direct determinations of critical-point energies with high accuracy.[4] In addition to this, it was also pointed out that these measurements can be especially sensitive to the surface quality of the sample. Small defect-containing regions of the sample surface or at the interface can produce strong electroreflectance signals which give rise to a critical-point energy and linewidth not representative of the bulk material.[5,6]

Even if some of these technical problems related to standard derivative measurement techniques are solved, differential optical spectroscopies still provide limited information about semiconductor band structures. In particular, the total signal is the result of transitions coming from throughout the Brillouin zone, rather than from a specific and well-defined point in $\mathbf{k}$ space. Optical spectroscopy cannot be used to measure the band dispersion. In addition to that, optical spectroscopy can provide accurate transition energies only between valence and conduction bands but cannot, in general, determine the absolute energy position of critical points with respect to a reference energy, e.g., the valence-band maximum.

An experimental technique capable of determining absolute critical-point energies and the dispersion $E(\mathbf{k})$ of valence bands is angle-resolved photoelectron spectroscopy (ARPES). During the last decade, ARPES has proven itself to be a very powerful experimental technique for investigating the bulk and surface electronic band structures of solids. Due to the interplay of several factors, such as (i) the availability of high-quality crystals, (ii) the minor contamination problems of some clean semiconductor surfaces under ultrahigh-vacuum conditions, and (iii) the presence of only a few valence bands with relatively strong dispersions, ARPES was very successful in the investigation of group IV, II-VI, III-V, and IV-VI compound semiconductors.[7–13] For a review about more recent ARPES experiments investigating surface and bulk electronic properties of semiconductor surfaces and interfaces, see Ref. 14.

In this paper, we report on normal-emission ARPES data from CdTe(100). The strong photon energy dependence of the spectral features from the top of the valence-band region allow us to determine the spin-orbit splitting $\Delta\varepsilon_{s.o.}$ unambiguously, as well as the width of the split-off band and the dispersion of the valence bands along the [100] direction. Our measurements also provide clear evidence of a $\sim$1-eV gap between the $\mathbf{G}_{-200}$ and $\mathbf{G}_{+200}$ final-state bands at the Brillouin-zone center. The energy of this gap is $\sim$11 eV above the valence-band maximum.

The measured spin-orbit splitting $\Delta\varepsilon_{s.o.}=0.95$ eV agrees to within our experimental uncertainty of ± 25 meV with earlier electroreflectance and photolumines-

cence measurements.[15,16] The experimentally determined dispersion of the heavy- and light-hole valence bands agrees well with predictions based on nonlocal pseudopotential calculations. For the width and dispersion of the split-off valence band, however, we find a small but noticeable discrepancy with theoretical predictions.[3,17] Our data imply a width of 4.4 eV, whereas a nonlocal pseudopotential calculation predicts a width of 5.05 eV. A comparison of the experimentally determined critical-point energies with results of various band-structure schemes indicates that the dispersion of the split-off valence band is generally overestimated in all model calculations.

II. EXPERIMENT

The photoemission experiments were performed at the University of Wisconsin's 1-GeV electron storage ring Aladdin. A Seya-Namioka beamline was used to provide monochromatic synchrotron radiation in the energy range $h\nu=9$–32 eV. The experimental setup consisted of a hemispherical sector analyzer mounted on a two axis goniometer. The total angular acceptance of the electron analyzer was 1.5°. The experimental energy resolution has contributions from both the monochromator and the electron analyzer. The total combined resolution as determined by the width of the Fermi level emission from the metallic clips of the sample holder was 0.15 eV at the high-energy photon end of the range, and slightly better at the low-energy end of the accessible photon energy range. Electron binding energies in this paper are referred to the Fermi level. All photoemission spectra were taken with the incident light 60° from the sample normal, and the analyzer positioned along the sample normal. The base pressure of the photoemission chamber was better than 1×10^{-10} torr.

The CdTe single crystal was 10×10 mm^2 in size and 1 mm in thickness, with the surface normal oriented along the [100] direction. The sample had been mechanically polished and chemically etched before insertion into the UHV system. Sputtering with 1-kV Ar^+ ions for two hours and annealing up to 280 °C for 30 min produced atomically clean and well-ordered surfaces.[18] After the final UHV cleaning cycle, the sample showed photoemission core spectra which were free of features characteristic of an oxidized and contaminated CdTe surface. In addition to that, the normal-emission valence-band spectra showed strong dispersive structures which are also an indication of an atomically clean and highly ordered surface.

During the cleaning cycles we monitored the improvement of the structural properties of the CdTe sample by reflection high-energy electron diffraction (RHEED). Figure 1 shows an intensity profile of a single line from a digitized RHEED image consisting of a total of 480 lines with 640 pixels per line. The intensity distribution was measured along a line perpendicular to the [100] sample normal with an electron energy of $E_0=20$ kV. The electron angle of incidence was ~2° with respect to the surface plane of the sample pointing along the [011] azimuth.

The line profile shows strong reflection peaks originating from the (00) reflected beam as well as the $(0\bar{1})$ and (01) lattice points. Weaker fractional-order peaks which are located between the main diffraction peaks are caused by a reconstruction of the surface which has the periodicity of two lattice constants for the direction perpendicular to the [011] azimuth. Previous work by Ebina and Takahashi reports a 3×1 and a faceted 1×1 reconstruction for CdTe(100) surfaces after different thermal treatment of the sputtered samples.[19] The difference in the observed reconstruction is most likely caused by different annealing conditions. In previous experiments with CdTe substrates we observed modifications in the reconstruction as well as in the surface chemistry for annealing temperature above ~320 °C.

III. RESULTS AND DISCUSSION

Figure 2 shows a selection of normal-emission valence-band spectra of CdTe(100). As one can see from Fig. 2, the emission features from the upper part of the valence-band emission are very sensitive to the selected excitation energy. For $h\nu=9$ eV the valence-band emission is relatively weak and unstructured, while for $h\nu=10$ eV the valence-band spectrum consists of a single strong and sharp emission feature. Increasing the photon

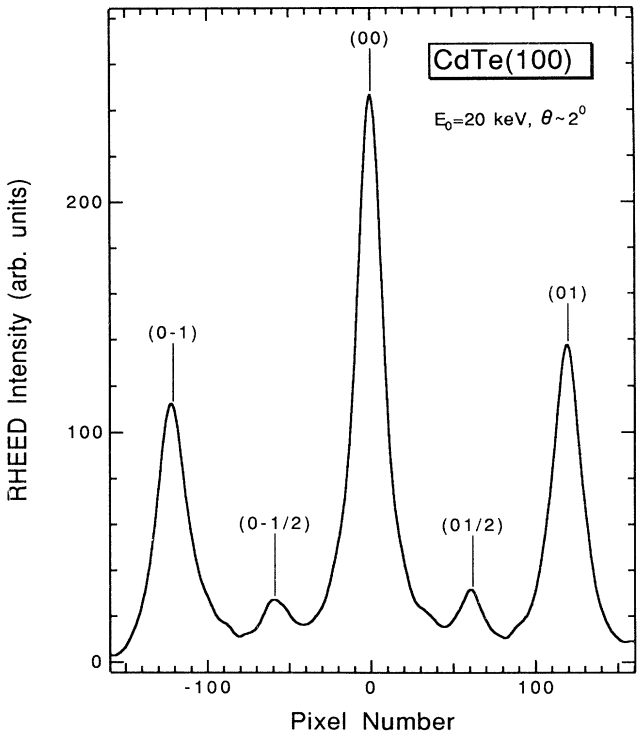

FIG. 1. RHEED intensity profile of CdTe(100) surface along the [011] azimuth. The kinetic energy was $E_0=20$ keV and the angle of incidence ~2°.

energy by another volt adds a second feature to the upper part of the valence-band spectrum and slightly disperses the leading peak further back into the valence band.

The dispersion of the two valence-band peaks continues with increasing photon energy as can be seen from the spectrum taken with $h\nu=16$ eV, which is displayed in the upper part of Fig. 2. Excitation with 16 eV photons also opens an additional transition channel which appears in the valence-band spectrum as a third peak located between the two initial structures. The appearance of new photoemission structures with increasing photon energy can easily be explained by direct transitions from the valence bands at the Γ point. Figure 3 shows schematically the direct transitions (e.g., $k_{\parallel}=0$) which contribute to the normal-emission valence-band spectrum characteristic for a spin-orbit zinc-blende-type semiconductor. In order to understand the sequence of emission features developing with increasing photon energy, it is not necessary to know the exact shape of the final-state bands E_f. However, as we will demonstrate later in the paper, the nearly-free-electron approximation of the final-state bands does describe our data reasonably well over most of the Brillouin zone. The only noticeable deviation from the free-electron-like band can be observed in the vicinity of the Brillouin-zone boundaries. The reason for these deviations is the periodic crystal potential which causes the bands to split at the boundary and to open an energy gap.

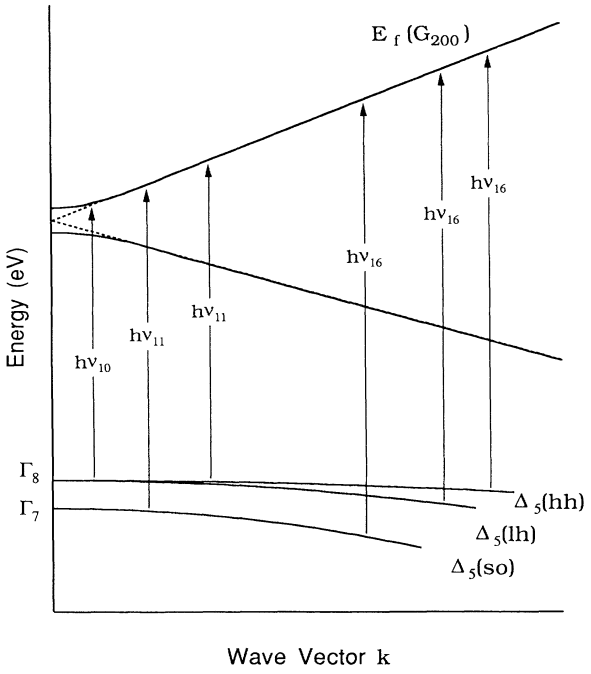

FIG. 3. Direct transition scheme describing the normal-emission angle-resolved photoemission transitions evolving from the heavy-hole (hh), light-hole (lh), and split-off (s.o.) valence band into the G_{200} final-state band.

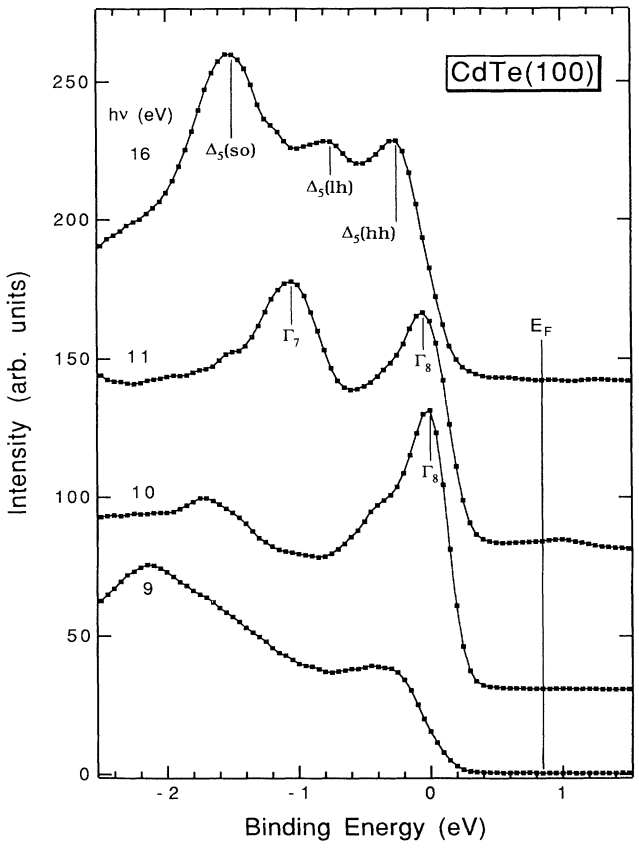

FIG. 2. Normal-emission valence-band spectra of CdTe(100). The spectra were measured with photon energies around the onset of transitions from the valence-band maximum at Γ_8.

The presence of the final-state gap which we have included in Fig. 3 can directly be seen in the valence-band spectra measured with low photon energies. In agreement with the data shown in Fig. 2, one can argue that the energy between the Γ_8 valence-band level and the final-state band near the zone center ($k\sim0$) is ~10 eV. Consider the bottom spectrum in Fig. 2 which was measured with $h\nu=9$ eV. This photon energy is too small for transitions from either the Γ_7 or Γ_8 levels to the upper branch of the final-state band. However, it is also too large to cause transitions to the lower branch of the final-state band. As a consequence of the final-state gap, there is no strong emission feature in the spectrum which could be traced back to direct transitions. The remaining much weaker features present in the spectrum result from nonprimary cone and indirect emission. Based on the absence of strong direct transitions in the photon energy range $h\nu\sim9$–10 eV, we estimate the final-state band-gap width to be ~1 eV.

Increasing the photon energy to $h\nu=10$ eV leads to a sharp peak which we have identified as the valence-band maximum Γ_8. It is at this energy that a transition from

the Γ_8 level to the final-state band just becomes possible. Increasing the photon energy to $h\nu=11$ eV forces the transitions to come from the slightly downward dispersing branch of the Δ_1 band away from the Γ_8 point. Since the initial-state band starts out with a very weak dispersion, photoemission features appear to remain constant in energy while the photon energy increases. The derivative of the valence-band spectrum, however, is very sensitive to small energy shifts and does clearly indicate the onset of the dispersion as can be seen in Fig. 4 where we display the numerical second derivatives d^2N/dE^2 of spectra measured with $h\nu=10$, 12, and 13 eV. The most striking observation is the appearance of emission associated with the Γ_7 level. This is as it should be, since now the photon energy is just large enough to cause a transition from Γ_7 to the final-state band.

From the distance in energy between the Γ_8 and Γ_7 levels in the $h\nu=10$ and 12 eV spectrum, we can directly measure the spin-orbit splitting. Figure 4 shows the second derivative of the spectra, from which we measured the spin-orbit splitting to be $\Delta\varepsilon_{sb}=0.95$ eV. Note that our conclusion that these two features indeed represent the Γ-point splitting and are not related to emission averaged over a section of the Brillouin zone relies only on the existence of a final-state band with a gap, but not on its specific shape. Also, the Γ_8 level has not started to disperse at a photon energy of $h\nu=11$ eV, as we could easily tell by comparing photoemission spectra taken with slightly higher photon energy. The spin-orbit splitting as determined by ARPES is in reasonable agreement with optical measurements of CdTe.[15,16,20]

Further increases in the photon energy are equivalent to mapping transitions along the [100] direction towards the X point in the Brillouine zone. The top curve of Fig. 3 shows a normal-emission spectrum taken with a photon energy $h\nu=16$ eV. At this excitation energy, emission arises from approximately one-tenth the distance to the X point, as we will prove later in the paper. This transition is far enough away from the zone center so that the Γ_8 level has split into two Δ_5 levels which are clearly

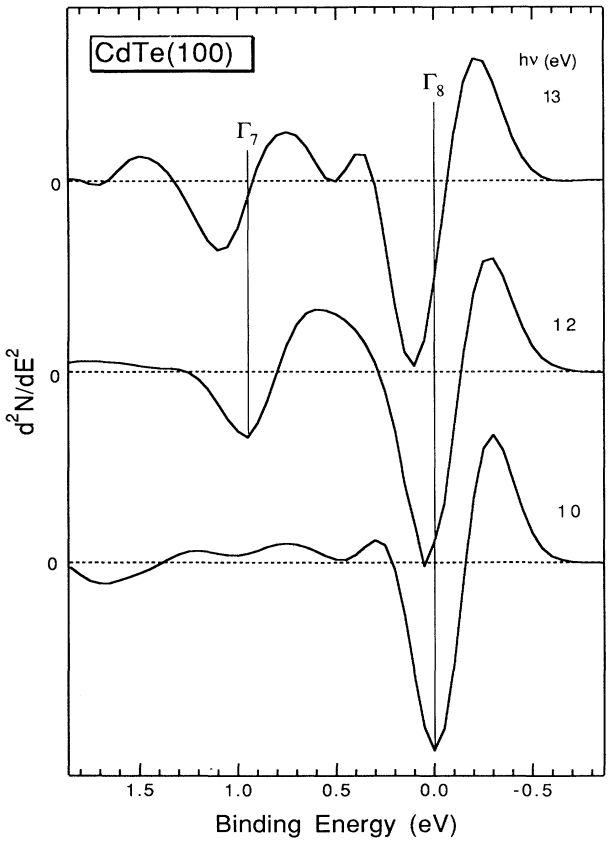

FIG. 4. Second derivative of selected normal-emission valence-band spectra of CdTe(100). The spin-orbit splitting $\Gamma_8-\Gamma_7=0.95$ eV is determined from the spectra measured at $h\nu=10$ and 12 eV. Note that for $h\nu=12$ eV the Γ_8 valence band starts to disperse away from the valence-band maximum while the Γ_7 state can contribute to the emission.

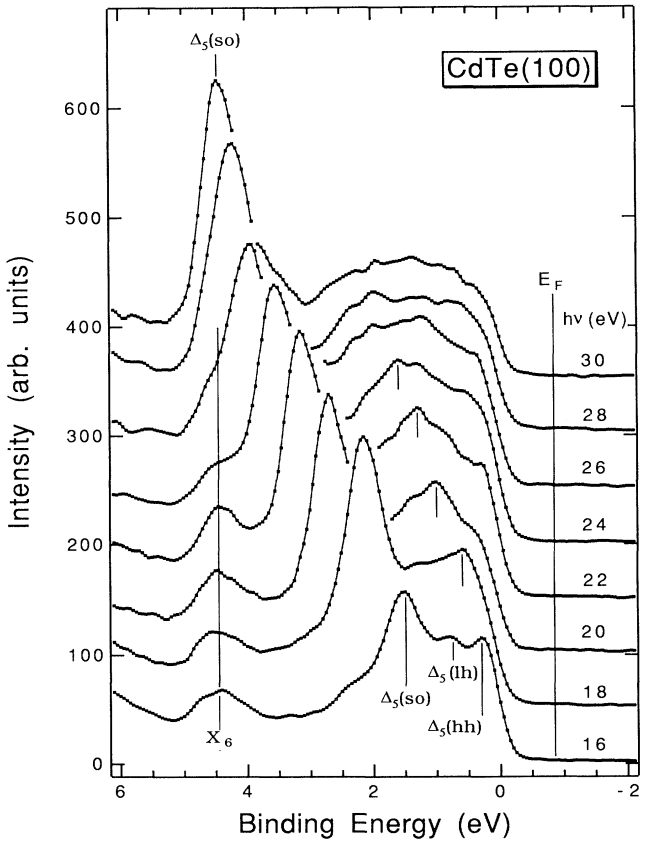

FIG. 5. Normal-emission valence-band spectra of CdTe(100). For excitation energies ranging from $h\nu=16$ to 30 eV the split-off Δ_5 band disperses over the whole Brillouin zone. Note the persistence of photon energy independent emission at $\sim$4.4 eV which is caused by indirect transitions from a high-density-of-state region around the critical valence-band point X_6.

resolved as two peaks, followed by a third originating from a strong direct transition from the remaining Δ_5 valence band.

The dispersion of valence-band features over larger sections of the Brillouin zone is summarized in Fig. 5 where we show a selection of normal-emission valence-band spectra taken with photon energies in the range $h\nu=16$–30 eV. While for $h\nu=16$ eV the direct transitions occur from near the zone center at Γ, emission is almost from the zone boundary at the X point for direct transitions excited with $h\nu=30$ eV. With increasing photon energy we also note a relative increase in the transition probability from the split-off band with respect to the transitions from the heavy- and light-hole bands throughout the entire Brillouin zone.

The observed drop in intensity for transitions away from the Γ point is a consequence of selection rules.[21,22] If one were to ignore the spin-orbit perturbation, then the appropriate point group for the crystal is T_d. The Γ_8 and Γ_7 levels which we have been discussing collapse into a triply degenerate Γ_4 level. Along the [100] direction, the nonzero k vector reduces the effective point group to C_{2v}, which has nondegenerate levels Δ_1 through Δ_4. The operator associated with the transition is the dipole operator $\mathbf{A}\cdot\mathbf{p}$, which has Δ_1 symmetry in C_{2v} for all polarizations of the incident electric field.

The final-state band is free-electron-like, and also has Δ_1 symmetry in C_{2v}. Therefore the only band along the [100] direction with a nonzero transition probability is the Δ_1 band, which is the one with the strongest dispersion. The inclusion of the spin-orbit interaction changes the symmetry and thus the nomenclature of this argument from single group to double group notation. The underlying physics, however, is not changed. All bands assume Δ_5 symmetry and the strongest dispersing is the split-off band with the highest transition probability.

To determine the dispersion relation $E(k)$ of the valence-band features we assumed a direct transition model with a free-electron-like final-state band. In a previous ARPES study of the CdTe(110) surface[18] we found that the normal-emission valence-band spectra could be modeled with a simple parabolic band $E_f=(h^2k_f^2/8\pi^2m)-E_0$. The energy offset E_0, which represents the bottom of the muffin-tin potential for electrons inside the crystal, is measured with respect to the Fermi level. Using the free-electron-like-state bands, the initial-state electron momentum is easy to determine. For normal-emission spectra the perpendicular component of the initial-state wave vector is $k_i=[(8\pi^2m/h^2)(h\nu-E_i+E_0)]-G$, where $\mathbf{G}$ is a reciprocal-lattice vector.

For a (100) surface, $\mathbf{G}$ vectors with a parallel component $\mathbf{G}_\parallel=0$ which can contribute to the normal-emission spectrum are integer values of $\mathbf{G}_{\pm200}$. The most prominent features in the normal-emission spectra originate from $\mathbf{G}_\parallel=0$ transitions (primary cone emission). There is also a possibility of reciprocal wave vectors with $\mathbf{G}_\parallel\neq0$ (surface umklapp and secondary cone emission) to contribute to the normal-emission spectrum. However, their intensity is significantly smaller and spectral structures arising from those transitions are easily distinguished from the direct, primary cone, emission features.

Figure 6 compares the experimentally determined band structure of CdTe along the ΓX direction with an empirical nonlocal pseudopotential calculation by Chelikowsky and Cohen (solid line) and with an energy-dependent semiempirical nonlocal scheme by Humphreys and Srivastava (dashed line).[3,23] The data points are from a fit of the experimentally determined initial-state energies to the final-state bands with an inner potential of $E_0=4.5$ eV which was determined as free fitting parameter. The free fit of the inner potential resulted in a value very close to what was independently determined by earlier ARPES from CdTe(110) surfaces.[24,18] As one can see from Fig. 6 there is good agreement between experiment and Chelikowsky and Cohen's calculation for the dispersion of the top two Δ_5 valence bands. The energy separation of the spin-off band is also quite accurately verified by the experimental data whereas the total width of the split-off band seems to be ~0.7 eV narrower than the theoretical

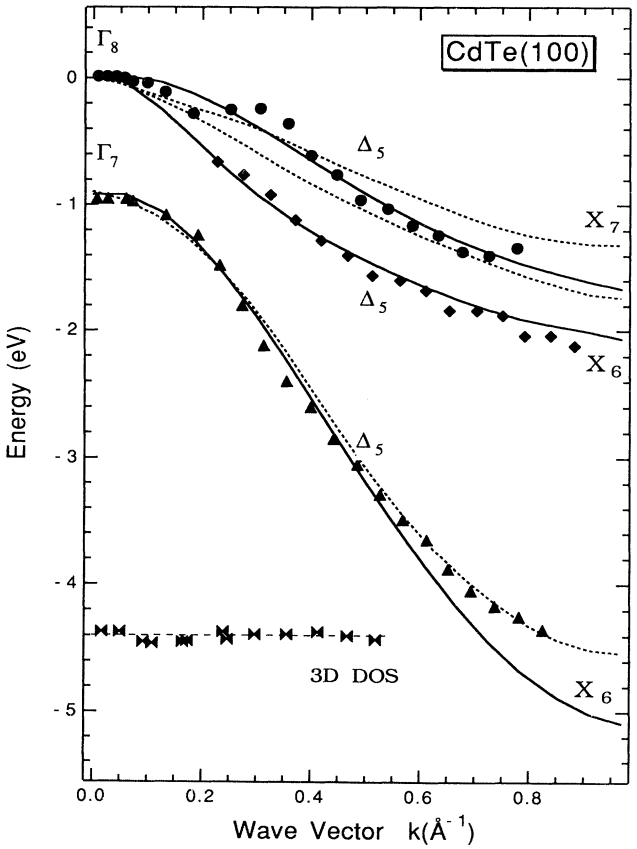

FIG. 6. Comparison of the experimentally determined valence-band dispersion $E(k)$ along the (100) direction of CdTe with band-structure calculations by Chelikowsky and Cohen (solid line) and Humphreys and Srivastava (dashed line) (Refs. 3 and 23).

predictions. Compared to an earlier ARPES study of CdTe(110) by Silberman *et al.*[25] our data describe the region around the valence-band maximum much better. Differences in absolute binding energy of the order of ~ 0.5 eV are easily caused by either not determining the critical-point energy by means of a closely selected set of photon energies or as in the case of Silberman *et al.* by placing the zero of the initial-state energy to the onset (leading edge) of the angle-resolved valence-band emission.

The presence of a nondispersive valence-band feature at ~ 4.4 eV binding energy which can be explained by indirect transitions from a region of high density of states around the X_6 point does provide strong additional support for our experimental findings of an overestimation of the dispersion of the third CdTe valence band in Chelikowsky and Cohen's nonlocal pseudopotential scheme. Our observation is not singular but seems to be of a more general nature typical to the special choices of nonlocal potential variation. Disagreement with the predicted dispersion and energy position of the third valence band was observed for several zinc-blende semiconductors including InSb and GaAs.[11,26,10]

It was suggested that the apparent shortcomings in predicting the absolute energy position and dispersion relation within the nonlocal pseudopotential theory could be improved by including a nonlocal d-well potential. Humphreys and Srivastava used an energy-dependent nonlocal pseudopotential scheme where they included a one-parameter anion d-well term.[23] The inclusion of the energy-dependent nonlocal corrections for both the s and d term in the potential does modify the energy position as well as the dispersion of the valence band. Humphreys and Srivastava's band structure (dashed line in Fig. 6) was calculated by including the above-mentioned effect of a nonlocal energy correction term. The incorporation of the correction term reduces the dispersion of the third valence band and describes the experimentally determined band dispersion of the third valence band much better.

However, the narrowing of the valence-band dispersion does not seem to be restricted to the split-off band, but also diminishes the light- and heavy-hole valence-band width. The critical point energies for the X_6 and X_7 valence-band level are ~ 0.3 eV smaller than those calculated by Chelikowsky and Cohen. The discrepancy between the experimental data and the calculated dispersion of these bands is quite obvious and seems to be of a more general nature inherent to the characteristics of the calculation method.

A more recent attempt to describe the electronic structure of CdTe by means of a self-consistent local-density formalism was made by Cade and Lee.[17] While the calculated spin-orbit splitting $\Delta_{s.o.}=0.952$ eV and the energy position of the heavy- and light-hole valence band agree well within our experimental findings, the local-density approach still overestimates the width of the split-off band by ~ 0.32 eV. The fact that the width of the split-off band is overestimated by $\sim 8.5\%$ may be used as further input for additional correction terms in order to refine the calculation scheme. It should be noted that the local-density approach is very successful in analyzing the electronic structure of metals. However, in determining the band structure of semiconductors, the method is prone to still show some systematic shortcomings. For instance, due to the discontinuity of the self-energy at the semiconducting gap, calculated band gaps tend to be significantly smaller than experimentally established gaps.

During the last years, several band-structure schemes were used to describe the bulk electronic properties of CdTe. Without going into the details of the special merits of the individual approaches, a general statement about their validity can be made. Even though they all claim satisfactory general agreement with nonlocal pseudopoential calculations, optical data, and density-of-state features derived from x-ray and angle integrated UV-photoemission spectra, they fail to predict the dispersion and absolute energy position of several high-symmetry points in the valence band. Table I compares selected high-symmetry valence-band energies of several band-structure schemes with values obtained from the present ARPES and optical measurements of CdTe.

It should be mentioned that the ARPES measurements are performed at ~ 300 K while band-structure calculations represent critical-point energies at 0 K. Optical data are usually measured at low temperatures and can thus be directly used for a comparison. In order to account for the higher temperature in the ARPES measurements one should correct the results against the temperature-dependent shift of the band structure. However, according to temperature-dependent photoluminescence spectra of CdTe as well as temperature-dependent measurements of the dielectric function of related zinc-blende compound semiconductors the ARPES valence-

TABLE I. Comparison of selected theoretical and experimental valence-band critical-point energies of CdTe. Energies are referenced against the valence-band maximum at $\Gamma_8=0$ eV.

Method	Γ_7	X_7	X_6	X_7
NPM[a]	−0.89	−1.60	−1.98	−5.05
SENPM[b]	−0.89	−1.30	−1.64	−4.54
TBM[c]	−0.93	−1.25	−1.71	−3.29
CPA[d]	−0.92	−1.57	−2.00	−5.02
SLD[e]	−0.95	−2.03	−2.40	−4.72
ARPES[f]	−0.95	≤ -1.40	−2.2	−4.40
ERS[g]	−0.91			
TS[h]	−0.945			
PLS[i]	−0.94			

[a]Nonlocal pseudopotential method, Ref. 3.
[b]Semiempirical nonlocal pseudopotential method, Ref. 23.
[c]Tight-binding method, Ref. 31.
[d]Coherent-potential approximation, Ref. 32.
[e]Self-consistent local-density method, Ref. 17.
[f]Angle-resolved photoemission spectroscopy, present paper.
[g]Electroreflectance spectroscopy, Ref. 15.
[h]Transmission spectroscopy, Ref. 20.
[i]Photoluminescence spectroscopy, Ref. 16.

band critical points are shifted by not more than ~50 meV towards smaller energies.[16,27,28] The thermally induced shift is within our experimental uncertainty and thus not worth correcting for.

IV. CONCLUSIONS

The present paper shows that synchrotron-radiation ARPES of CdTe(100) is very useful to map critical-point energies as well as the dispersion $E(k)$ of valence bands. Even though photoemission spectroscopy cannot compete with the higher-energy resolution intrinsic to optical spectroscopy, derivative techniques combined with the availability of finely tuned synchrotron radiation allow ARPES to provide valuable information to serve as critical reference for future correction terms to be added in improved band-structure calculations.

Advancements in the photoemission instrumentation as well as in sample preparation and data analysis allow ARPES measurements of high precision which could be utilized for a more rigorous comparison with theoretical predictions. Instead of adjusting empirical tight-binding calculations so that they fit the experimental data, as done in the case of GaAs, it may be of greater general interest to point out discrepancies of ARPES results with current state of the art calculations.[29,30] In that regard it would be of special help, if theoreticians treat these experimental efforts as a critical test of their models.

However, one should also note that we compare theoretical one-electron properties with results obtained by an excitation spectroscopy and some of the observed discrepancies may well be related to many-body effects. Angle-resolved photoemission from nearly-free-electron metals indicates a band-gap narrowing which can be directly linked to the electron density by considering the quasiparticle self-energy term.[33] At a typical electron density of $\sim 3\times 10^{22}$ electrons/cm^3, the observed band width narrows by ~0.7 eV.

Unfortunately our present understanding of how these many-body effects may modify the one-electron properties of semiconductors has not yet developed. The presently used framework of the interacting electron gas[34] is most likely not suitable for a study of many-body effects in tetrahedrally coordinated semiconductors. However, considering the fact that carrier densities in a typical semiconductor are several orders of magnitude smaller than in a free-electron metal, one may expect a minor correction of the single-particle energy $E(\mathbf{k})$ by the quasiparticle self-energy term $\Sigma(\mathbf{k},E)$.

ACKNOWLEDGMENTS

The authors would like to thank the staff of the Synchrotron Radiation Center for technical support and M. A. Engelhardt for his assistance with the experimental setup. D.W.N. would also like to acknowledge support from the Alexander von Humboldt Foundation while the actual experiments were in progress.

[1]M. Cardona, *Modulation Spectroscopy* (Academic, New York, 1969), Suppl. 11.
[2]F. Herman, R. L. Kortum, I. B. Ortenburger, and J. P. van Dyke, J. Phys. (Paris) Colloq. **29**, C4-62 (1968).
[3]J. R. Chelikowsky and M. L. Cohen, Phys. Rev. B **14**, 556 (1976).
[4]J. W. Garland, C. Kim, H. Abad, and P. M. Raccah, Phys. Rev. B **41**, 7602 (1990).
[5]L. Kassel, H. Abad, J. W. Garland, P. M. Raccah, J. E. Potts, M. A. Haase, and H. Cheng, Appl. Phys. Lett. **56**, 42 (1990).
[6]P. M. Raccah, J. W. Garland, Z. Zhang, L. L. Abels, S. Ugur, S. Mioc, and M. Brown, Phys. Rev. Lett. **55**, 1323 (1985).
[7]R. I. G. Uhrberg, G. V. Hansson, U. O. Karlsson, J. M. Nicholls, P. E. S. Persson, S. A. Flodström, R. Engelhardt, and E. E. Koch, Phys. Rev. B **31**, 3795 (1985).
[8]R. D. Bringans and H. Höchst, Phys. Rev. B **25**, 1081 (1982).
[9]T. Grandke, L. Ley, and M. Cardona, Phys. Rev. B **18**, 3847 (1978).
[10]T. C. Chiang, J. A. Knapp, M. Aono, and D. E. Eastman, Phys. Rev. B **21**, 3513 (1980).
[11]H. Höchst and I. Hernández-Calderón, Surf. Sci. **126**, 25 (1983).
[12]I. Hernández-Calderón, H. Höchst, A. Mazur, and J. Pollman, J. Vac. Sci. Technol. A **5**, 2042 (1987).
[13]K. O. Magnusson and S. A. Flodström, Phys. Rev. B **38**, 1285 (1988).
[14]R. D. Bringans, *Angular-Resolved Photoemission* (Elsevier, New York, 1990).
[15]M. Cardona, K. L. Shaklee, and F. H. Pollak, Phys. Rev. **154**, 696 (1967).
[16]D. J. Olego, J. P. Faurie, and P. M. Raccah, Phys. Rev. Lett. **55**, 328 (1985).
[17]N. A. Cade and P. M. Lee, Solid State Commun. **56**, 641 (1985).
[18]H. Höchst, D. W. Niles, and I. Hernández-Calderón, Phys. Rev. B **40**, 8370 (1989).
[19]A. Ebina and T. Takahashi, J. Cryst. Growth **59**, 51 (1982).
[20]A. Twardowski, E. Rokita, and J. A. Gaj, Solid State Commun. **36**, 927 (1980).
[21]J. Hermanson, Solid State Commun. **22**, 9 (1977).
[22]M. Tinkham, *Group Theory and Quantum Mechanics* (McGraw-Hill, New York, 1964).
[23]T. P. Humphreys and G. P. Srivastava, Phys. Status Solidi B **112**, 581 (1982).
[24]K. O. Magnusson, S. A. Flodström, and P. E. S. Persson, Phys. Rev. B **38**, 5384 (1988).
[25]J. A. Silberman, D. Laser, C. K. Shih, D. J. Friedman, I. Lindau, W. E. Spicer, and J. A. Wilson, J. Vac. Sci. Technol. A **3**, 233 (1985).
[26]A. McKinley, G. P. Srivastava, and R. H. Williams, J. Phys. C **13**, 1581 (1980).
[27]L. Viña, H. Höchst, and M. Cardona, Phys. Rev. B **31**, 958 (1985).
[28]L. Viña, S. Logothetidis, and H. Höchst, in *Proceedings of the 17th International Conference on the Physics of Semiconductors,* edited by James D. Chadi and Walter A. Harrison (Springer, New York, 1984), p. 1025.
[29]T. C. Chiang, R. Ludeke, M. Aono, G. Landgren, F. J.

Himpsel, and D. E. Eastman, Phys. Rev. B **27**, 4770 (1983).
[30]M. L. Cohen and J. R. Chelikowsky, *Electronic Structure and Optical Properties of Semiconductors,* Vol. 75 of *Springer Series in Solid-State Sciences,* edited by Manuel Cardona (Springer-Verlag, Berlin, 1988).
[31]M. T. Czyzyk and M. Podgorny, Phys. Status Solidi B **98**, 507 (1980).
[32]A. Chen and A. Sher, J. Vac. Sci. Technol. **21**, 138 (1982).
[33]E. W. Plummer, Phys. Scr. **T17**, 186 (1987).
[34]L. Hedin, Phys. Rev. A **139**, 796 (1965).